





# Chapter 1

## The T2K Experiment

The Tokai-to-Kamioka (T2K) experiment [1] is a long baseline neutrino oscillation experiment located in two sites across Japan and is designed to study the parameters governing the PMNS matrix. The first site is the J-PARC facility in Tokai-mura on Japan's east coast which houses a 30 GeV proton accelerator complex that is used to generate a highly pure  $\nu_\mu$  beam. J-PARC also contains a suite of detectors designed to measure the neutrino beam's unoscillated characteristics. Super-Kamiokande (SK) is located 295 km (see Fig. 1.1) and measures the contents of the neutrino beam post-oscillation.

T2K was the first experiment to observe the  $\nu_\mu \rightarrow \nu_e$  appearance channel [2] which excluded  $\theta_{13} = 0$  at  $7.3\sigma$  significance. By comparing this result with precise  $\theta_{13}$  measurements from reactor experiments,  $\delta_{CP}$  regions can be excluded at 90% confidence level (see Fig. 1.2). T2K's precision analysis of the  $\nu_\mu$  disappearance channel provide world leading measurements of  $\theta_{23}$  and  $\Delta m_{23}^2$ . Independently of the oscillation analyses performed by the experiment, T2K's near detectors, ND280 and INGRID, are used to measure a range of neutrino cross-sections [3,4]. While this is not the primary aim of T2K, such measurements are still extremely important as T2K systematic uncertainties

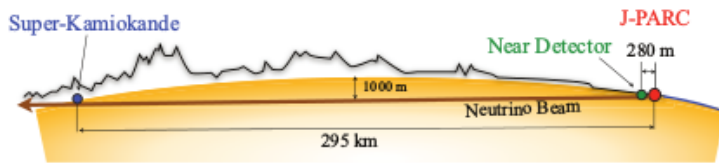


**Figure 1.1:** Schematic of the T2K experiment showing the near and far sites, separated by the 295 km baseline.

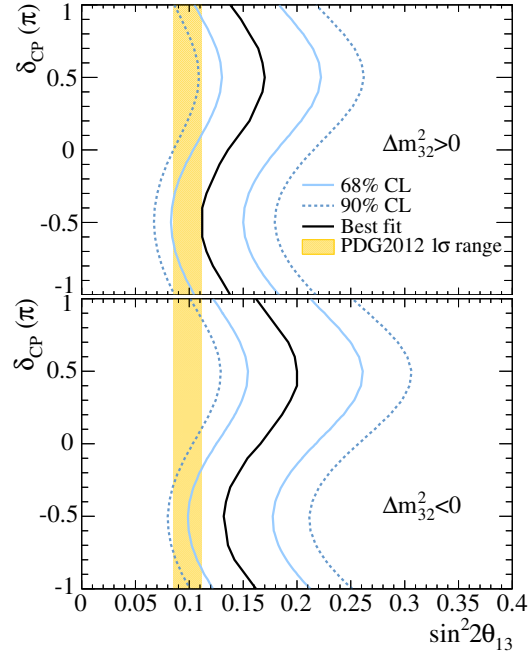


**Figure 1.2:** The 68% and 90% confidence level allowed regions for  $\sin^2 2\theta_{13}$  as a function of  $\delta_{CP}$  for normal hierarchy (top) and inverted hierarchy (bottom). The solid line represents the best fit  $\sin^2 2\theta_{13}$  for a given  $\delta_{CP}$ . The shaded region shows the average  $\theta_{13}$  provided by the reactor constraint [2].

can be constrained with additional cross-section knowledge as well as helping to understand the general neutrino interaction picture.

## 1.1 T2K beam

The T2K neutrino beam is generated by J-PARC's accelerator complex which produces a 30 GeV proton beam which is fired at a fixed graphite target. The final-state particles of interactions with the target are predominately charged pions which decay to produce the neutrino beam. Surrounding and behind the graphite target are a set of magnetic horns which focus the pions into a beam, resulting in a focused neutrino beam after the hadrons have decayed.



**Figure 1.3:** A schematic of the T2K neutrino beamline (left) and a side view of the secondary beamline (right) [1].

### 1.1.1 Accelerator complex

The J-PARC accelerator complex consists of three sections: the LINear ACcelerator (LINAC), the Rapid-Cycling Synchrotron (RCS) and the Main Ring synchrotron (MR). Production of the proton beam starts at the LINAC where  $H^-$  anions are accelerated to 181 MeV which are subsequently converted to  $H^+$  ions via charge-stripping foils at the RCS injection point. With a 25 Hz cycle, the ions are further accelerated by the RCS to 3 GeV with two bunches per cycle. Roughly 5% of the proton bunches are fed into the MR where the final acceleration to 30 GeV occurs in bunches of eight. Extraction of the bunches occurs at two points for different experiments. For T2K, all eight bunches are extracted in a single turn by five kicker magnets and aimed down the neutrino beamline to the graphite target. The extraction of all eight bunches forms a single beam spill with a width of 5  $\mu$ sec. The tight structure of the beam spills is vital for background discrimination in the downstream detectors.

### 1.1.2 Neutrino beamline

The neutrino beamline (NU) is split into a primary and secondary beamline, a schematic of which is shown in Fig. 1.3. The primary beamline consists of a preparation section, an arc section and a focusing section. The preparation section uses 11 normal conducting magnets to tune the proton beam for entry into the arc section where the proton beam is bent to its intended direction. As will be discussed in more detail in section 1.1.3, the axis of the beam is  $2.5^\circ$  away from SK. The final focusing sections then guides the proton beam into the secondary beamline and the graphite target.

Sound performance of the proton beam is vital for stability of the T2K neutrino beam. To ensure such performance, the primary beamline is equipped with a suite of monitors to measure the position, profile, loss and intensity of the proton beam. The beam position is measured by 21 ElectroStatic Monitors (ESMs) which consists of four cylindrical electrodes surrounding the beam. The asymmetry of the beam is measured by the induced current in the electrodes which is used to infer the position in a non-destructive manner. Segmented Secondary Emission Monitors (SSEMs) are used to measure the beam loss. Each SSEM has an anode foil sandwiched between two titanium foil strips. Protons interact with the strips causing an emission of electrons which electrically drift inducing a current in the strips. The charge distribution is used to reconstruct the profile. The Beam Loss Monitors (BLMs) are Ar-CO<sub>2</sub> filled wire proportional counters and are used to quantify the beam loss. The intensity of the beam is measured by five Current Transformers (CTs) which consist of a 50-turn toroidal coil around a ferromagnetic coil. Passage of the beam induces a current in the coil which is used to infer the number of protons in the spill. The final CT (CT5) is positioned at the end of the focusing section of the primary beamline and is used to count the number of protons incident on the graphite target. The accumulated number of protons on target (POT) is used as a metric for the data collected by T2K. The total POT accumulated so far by T2K is shown in Fig. 1.4.

The secondary beamline consists of the graphite target, a set of magnetic focusing horns, a decay pipe and a beam dump. A schematic for the secondary beamline is shown in Fig. 1.3. The graphite target is a 2.6 cm diameter and 91.4 cm long rod which is surrounded by a 2 mm thick graphite tube and a 0.3 mm titanium case. The proton-graphite interactions produce charged pions and kaons which are focused by three magnetic horns, one of which surrounds the target. The magnetic horns consist of two coaxial conductors which generate a magnetic field with a strength inversely proportional to the distance from the beam axis. The current direction in the magnetic horns causes the induced field to focus or deflect particles depending on their charge sign. This simple control allows T2K to operate in  $\nu$  or  $\bar{\nu}$  beam mode. The focused mesons then travel down a decay pipe filled with Helium to reduce pion absorption. It is here that the mesons decay to produce the neutrinos which form the T2K beam. To stop measurement contamination, other decay products must be stopped before reaching the downstream detectors. So, a 75 ton graphite beam dump is positioned at the end of the decay volume. The beam dump stops almost all non-wanted decay products, with only 5 GeV or above muons successfully propagating through. As the

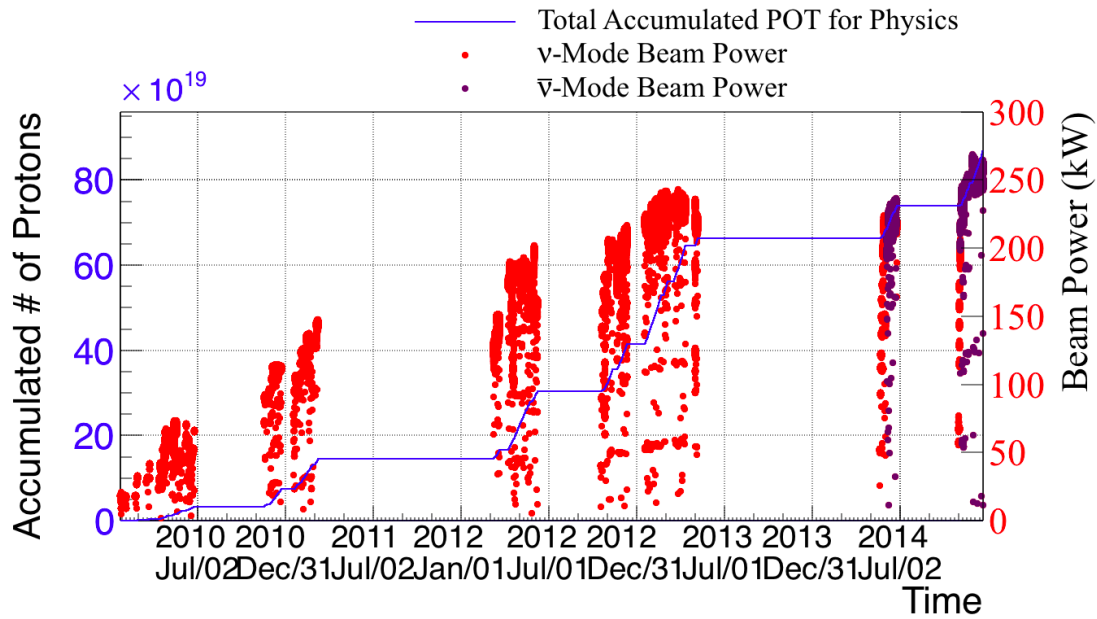


**Figure 1.4:** The POT recorded by CT5 as a function of time (blue line) and the recorded beam power in  $\nu$  running mode (red dots) and  $\bar{\nu}$  running mode (purple dots).

muons are generally simultaneously produced with the beam neutrinos, measurements of the muons can be used to monitor the direction of the neutrino beam. To do this, a MUon MONitor (MUMON) is installed at the downstream end of the beam dump.

### 1.1.3 Off-axis beam

The kinematics of the pion decays dictate the energy spectrum shape of the neutrinos. Specifically, the peak width of the neutrino energy narrows and shifts as an observer moves off-axis from the pions trajectory. As the pions are the neutrino parents in the T2K beam, the same effect can be seen by moving off-axis from the neutrino beam. This effect is illustrated in Fig. [?]. By positioning T2K's baseline detectors at  $2.5^\circ$  off-axis, it is possible to align the neutrino beam's peak energy with the first oscillation maximum for the  $\nu_\mu$  disappearance channel. Separately, an off-axis configuration reduces the beam's unwanted high energy tail, improving sensitivity to  $\nu_e$  appearance and  $\nu_\mu$  disappearance.

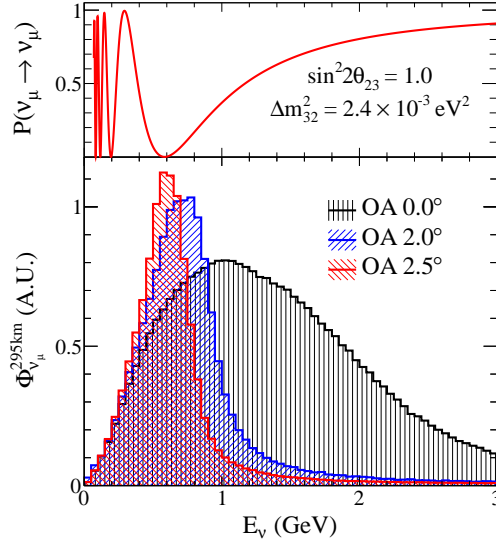


**Figure 1.5:** Muon neutrino survival probability at 295 km (top) and neutrino fluxes for different off-axis angles (bottom) [5]. The peak neutrino lowers and the energy distribution narrows as the off-axis angle increases.

## 1.2 Near detector complex

Located 280 m downstream of the beam target is the near detector complex which houses a pair of detectors which measure the unoscillated characteristics of the beam. The two detectors, named INGRID and ND280, sit in a 37 m deep, open air pit lined with concrete which is surrounded by sand.

### 1.2.1 Multi-Pixel Photon Counter

Multi-Pixel Photon Counters (MPPCs) [6] are used extensively in both INGRID and ND280 for detection of scintillation light during particle energy deposition in plastic scintillator. The choice of MPPCs, rather than more traditional photomultiplier tubes, was largely due to their ability to operate in a magnetic field. A MPPC is a multi-pixel avalanche photodiode which consists of 667 pixels over an area of  $1.3 \times 1.3 \text{ mm}^2$ . In terms of operation, each MPPC is held at 0.8-1.5 V above their breakdown voltage, resulting in a gain of  $1 \times 10^6$ , which is consistent with the gain of a vacuum photomultiplier [1]. When light is incident on a MPPC, each pixel acts as a detector for a single photon which means the total signal collected is simply the sum of the MPPC's fired pixels.



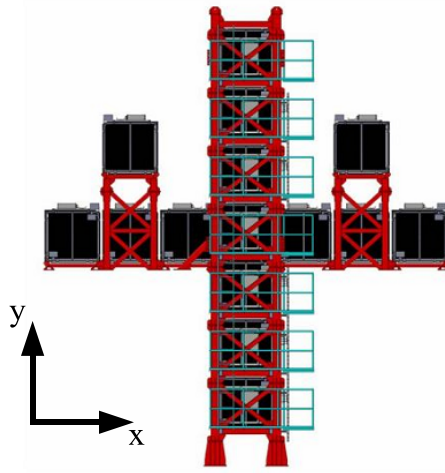


**Figure 1.6:** A schematic of INGRID [1].

The scintillator bars, which the MPPCs collect the light from, consist of plastic scintillator bars with a wavelength shifting (WLS) fibre threaded through the centre. During energy deposition, the plastic scintillator emits photons which are collected and transported by the WLS fibre to the bar's end where the MPPC is located. The WLS fibre has a twofold purpose: carry the light to the MPPC and shift the spectrum of the light to a region where MPPC detection is optimised.

### 1.2.2 INGRID

INGRID (Interactive Neutrino GRID) is one of T2K's near detectors. With its centre positioned on the beam axis, INGRID is designed to directly monitor the beam's direction and intensity. INGRID consists of 14 identical modules arranged in a cross formation with two additional modules positioned off the cross axis towards the end of each horizontal arm (see Fig. 1.6). The cross arrangement allows INGRID to sample the beam in a  $10\text{ m} \times 10\text{ m}$  transverse section.

Each module consists of nine iron plates and 11 tracking scintillator planes in a sandwich structure. The iron plates are  $124\text{ cm} \times 124\text{ cm} \times 6.5\text{ cm}$  and provide 7.1 tons of target per module for the neutrino beam. The scintillator planes provide tracking for the neutrino final-states and consist of scintillator bars threaded by WLS fibres and readout by MPPCs (see section 1.2.1).

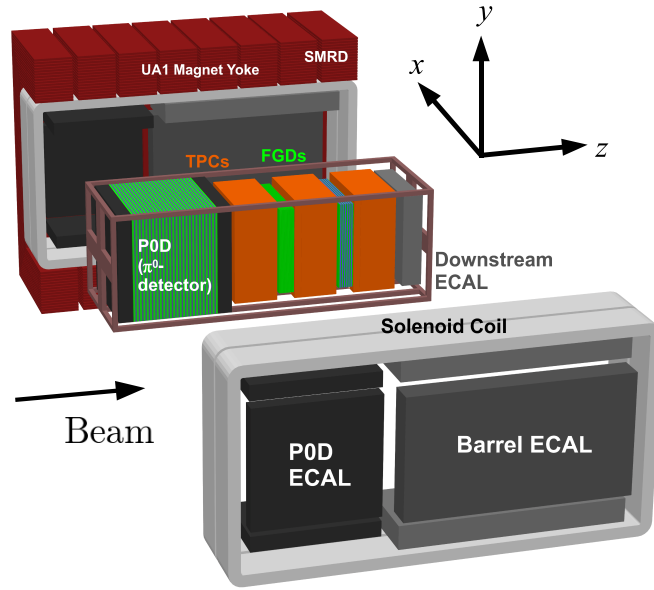


**Figure 1.7:** An exploded view of ND280 [1].

This overall design allows INGRID to measure the beam centre to a 10 cm precision which corresponds to 0.4 mrad precision at the near detector complex [1].

### 1.2.3 ND280

ND280 (Near Detector at 280 m) is T2K's other near detector. However, unlike INGRID, ND280 is positioned  $2.5^\circ$  off-axis to the neutrino beam. ND280 is a heavy, fine-grained detector which characterises the flux, energy spectrum and  $\nu_e$  contamination of the  $\nu_\mu$  beam and additionally makes neutrino cross-section measurements. Because ND280 sits at the same off-axis angle as T2K's far detector, ND280's beam characterisation can be used to make signal and background predictions at the far detector.

Fig. 1.7 shows an exploded view of the detector, which reveals the many subdetectors that form ND280. The central tracking region comprises two Fine-Grained Detectors (FGDs [7]) sandwiched between three Time Projection Chambers (TPCs [8]). The FGDs, which are composed of layers of plastic scintillator bars, provide the primary target for the neutrinos to interact with and the TPCs, filled with a gaseous mixture, allow for tracking of the charged final-states. Essentially, the detectors in this region are complimentary and their combined information is used to reconstruct the majority of beam events relevant for oscillation analyses. Upstream of the tracker

region lies the  $\pi^0$  detector (PØD [9]), whose design is optimised for studying neutrino interactions with  $\pi^0$  in the final-state and consists of layers of scintillator, water and brass. Surrounding the tracker and PØD are a set of Electromagnetic Calorimeters (ECals [10]), primarily designed to detect particles originating from ND280's inner region. Because particle identification is paramount to ND280's physics goals, all of the above detectors sit in a constant 0.2 T magnetic field, which is aligned with the  $x$ -axis in Fig. 1.7. The magnetic return yoke and coils used to generate this field encompass the entire detector, allowing a constant field to be maintained within the detector, but greatly minimising the field's outside extent. To maximise ND280's physics capability, the magnetic return yoke is instrumented with layers of plastic scintillator, which form the Side Muon Range Detectors (SMRDs [11]).

### 1.2.3.1 The electromagnetic calorimeters

The ND280 ECal is a lead-scintillator sampling calorimeter which consists of 13 modules separated into three distinct regions: the PØD ECal which consists of six modules surrounding the PØD, the barrel-ECal which is separated into six modules surrounding the tracker region and the DownStream-ECal (DS ECal) which is a single module located downstream of the inner detectors. Motivated by their physics goals, the barrel-ECal and DS ECal are often considered together and will be referred to as the tracker ECal, while the PØD ECal is considered a separate detector which is not used in this analysis and so will not be discussed further. The primary physics goal of the ECal is to aide particle identification for final-states originating in the central region of ND280. This is particularly important for interactions with  $\pi^0$  in the final-state as the decay photons are difficult to identify using the tracker alone.

The barrel-ECals are separated into six modules: two modules above the tracker, two either side of the tracker and two below the tracker. Each barrel-ECal module consists of layers of scintillating polystyrene bars with a 40 mm  $\times$  10 mm cross-section bonded to 1.75 mm lead sheets. The scintillator bars provide a means of tracking the final-states while the lead sheets act as a radiator to produce electromagnetic showers and additionally provide a heavy mass neutrino target. To measure the light readout, each scintillator bar has a 2 mm hole running through the centre in which a WLS fibre is inserted. The fibre carries the light to the end of the bar where it can be collected by an MPPC. The size of the gap between the tracker and the magnet placed a strong constraint on the size of barrel modules and so a scintillator bar thickness

of 10 mm was chosen to minimise the ECal depth while maintaining a bar thickness which could provide sufficient light for signal capture. The other key features of the active barrel-ECal volume (bar thickness, lead thickness and number of layers) were chosen to optimise particle identification and tracking. A smaller bar width results in a detector with a higher resolution and studies investigating this found that the  $\pi^0$  reconstruction efficiency was greatly compromised for  $>50$  mm bar widths. So, to facilitate costings, a compromise bar width of 40 mm was chosen. The thickness of the lead absorber was also optimised based on the  $\pi^0$  reconstruction efficiency. The number of scintillator-lead layers was chosen such that electromagnetic showers of energy up to 3 GeV were adequately contained. It was found that 10 electron radiation lengths ( $X_0$ ) were required to ensure containment of at least 50% of  $\pi_0$  decay photon showers. So, this motivated a choice of 31 layers for all barrel-ECal modules which is equivalent to  $9.7X_0$ . For the purpose of 3D reconstruction, each ECal layer is oriented at  $90^\circ$  to the previous layer. This means that in all barrel modules, there are 16 layers perpendicular and 15 layers parallel to the beam direction. The perpendicular and parallel layers are slightly different, in that the scintillator bars are a different length. In all barrel modules, the parallel bars are 3840 mm and are read out at both ends by separate MPPCs. Because of the geometry, this is not the case for the perpendicular bars; the top and bottom module bar lengths are 1520 mm whereas the side module bar lengths are 2280 mm. For all perpendicular bars, the signal is read out at one end only with the other end mirrored with aluminium to reflect the light. Each barrel module is sandwiched between two carbon fibre plates and held in an aluminium frame which provides secure, structural support.

The DS ECal has almost identical features to that of the barrel in that it has scintillator bars with an identical chemical composition and cross-section while the lead absorbers are equally thick. However, unlike the barrel-ECals, the DS ECal consists of 34 lead-scintillator layers which are, again, orientated at  $90^\circ$  to the previous layer. Because of this, the DS ECal has a radiation length of  $10.6X_0$ . Additionally, every scintillator bar is 2000 mm and is read out at both ends by MPPCs. Also, because of its position in the geometry, all layers are perpendicular to the beam direction. The carbon fibre plates and aluminium frame are identical to those used in the barrel-ECal.

A summary of the tracker ECal design is shown in table. 1.1.

	DS ECal	Barrel ECal
Length (mm)	2300	4140
Width (mm)	2300	1676 top/bottom 2500 side
Depth (mm)	500	462
Weight (kg)	6500	8000 top/bottom 10000 side
Num. of layers	34	31
Bar orientation	$x/y$	Para. and Perp
Num. of bars	1700	2280 Para. top/bottom 1710 Para. sides 6144 Perp top/bottom 3072 Perp sides
Bars per layer	50	38 Para. top/bottom 57 Para. side 96 Perp top/bottom/sides
Bar length (mm)	2000	3840 Para. 1520 Perp top/bottom 2280 Perp sides
Pb thickness (mm)	1.75	1.75

**Table 1.1:** Summary of the ECal design showing the overall dimensions, numbers of layers, length and orientation of the scintillator bars, numbers of bars, and lead thickness for each module [10].

The scintillator bars consist of polystyrene doped with 1% PPO and 0.03% POPOP and were extruded at a dedicated Fermilab facility. During charge deposition, the PPO works as the primary scintillator and its output photons result in secondary scintillation of the POPOP. This process acts as a wavelength shifter to produce an emission peak of 420 nm which matches the absorption peak of the 1 mm diameter WLS fibre threaded through the centre of the bar. Every tracker ECal bar contains a 0.25 mm coating of polystyrene co-extruded with  $\text{TiO}_2$  which provides reflection of the scintillation light.

The lead absorber layers consist of naturally occurring lead and stiffened with 2% antimony. Traces of other metals are present but are below 0.15%. During construction, each lead layer was coated with a black, quick drying metal-conditioning primer to protect personnel from the toxic effects of the lead and to prevent leaching into the scintillator bars. The lead layers themselves are actually constructed from multiple sheets rather than a single sheet largely due to ease of transportation. In the case of the DS ECal, each layer consists of two 1008 mm  $\times$  2016 mm sheets. For the top and bottom ECal modules, each layer consists of two 765 mm  $\times$  3858 mm sheets and the side module absorbers are constructed from four 2330 mm  $\times$  964.5 mm sheets.

The tracker ECal electronics system consists of several different readout boards. All MPPCs are connected to a set of bespoke Trip-T [12]<sup>1</sup> Frontend Boards (TFBs). Each TFB comes with 64 channels to read out MPPCs which means that there are multiple TFBs associated with each ECal module. All TFBs subsequently connect to Readout Merger Modules (RMMs) which act as the interface between the Data Acquisition system (DAQ) and its associated TFBs.

### 1.2.3.2 Data acquisition system

ND280 comes equipped with a DAQ which is responsible for triggering the readout of information from the subdetectors and subsequent storage. Because of the low frequency of neutrino events, there are no strict trigger requirements which is in stark contrast to collider experiments. So, there are only three triggers which are:

- **Beam trigger:** When a beam spill occurs, a timing signal is sent to the DAQ which issues a command to record ND280 data.

---

<sup>1</sup>ADDRESSED - Need a citation for the trip-t boards

- **TRIP-t cosmic trigger:** If hits are seen on opposite sides of the outer detectors (allowed combinations are top and bottom SMRD, left and right SMRD, PØD and DS ECal) which are outside of the beam time window, then the DAQ records data as the hits were likely caused by a cosmic ray muon.
- **FGD cosmic trigger:** If hits are seen in both FGDs which are outside of the beam time window, then data is recorded as this was also likely to be caused by a cosmic ray muon.

The data is initially stored at KEK in Japan but is then replicated to TRIUMF in Canada and RAL in the UK for maximum redundancy and ease of access.

#### 1.2.4 The far detector

The T2K experiment's far detector is Super-Kamiokande [13], which is a very large water Cherenkov detector containing 50 kton of ultra-pure water. Positioned 295 km away from the J-PARC neutrino beam, SK is located under Mt. Ikenoyama with a rock overburden of 1 km (2.7 km water-equivalent)<sup>2</sup>. SK consists of two detectors; the inner detector consists of 11,146 inward facing 20''<sup>3</sup> PMTs which surround 35,000 ton of water while the outer detector consists of 1,885 outward facing 8''<sup>4</sup> PMTs and acts as a veto for entering backgrounds.

SK detects particles via Cherenkov radiation which is produced as a result of charged particles travelling in excess of the speed of light in the local medium. This radiation is emitted at an angle of  $\cos \theta = c/nv$ , where  $n$  is the refractive index of the material and  $v$  is the speed of the particle. For water this equates to an angle of  $42^\circ$ . The medium imposes a damping effect on the velocity of the particle, which results in energy loss and there comes a point where the Cherenkov emission condition is no longer met. So, SK detects a ring of light emitted by the particles propagating through it.

The features of the Cherenkov ring are utilised for particle identification. An electron, which showers upon creation in the water, creates a fuzzy ring of light while a muon, which cleanly propagates through the water, creates a sharp ring of light. Examples of

<sup>2</sup>ADDRESSED - also put water equivalent

<sup>3</sup>ADDRESSED - was "

<sup>4</sup>ADDRESSED - was "

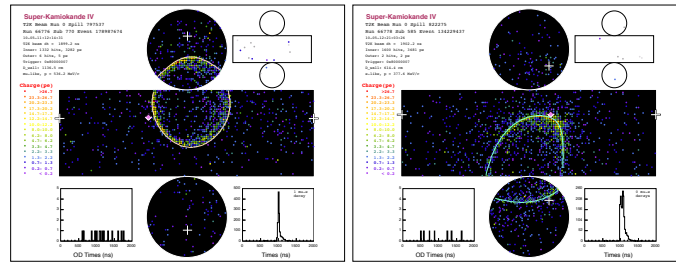


**Figure 1.8:** Example of reconstructed T2K events in SK for a muon-like ring (left) and an electron-like ring (right) [1].

this are shown in Fig. 1.8 where the difference between muon and electron events can be clearly seen.







# Bibliography

- [1] K. Abe *et al.*, Nuclear Instruments and Methods in Physics Research Section A: Accelerators, Spectrometers, Detectors and Associated Equipment **659**, 106 (2011).
- [2] (T2K Collaboration), K. Abe *et al.*, Phys. Rev. Lett. **112**, 061802 (2014).
- [3] (T2K Collaboration), K. Abe *et al.*, Phys. Rev. Lett. **113**, 241803 (2014).
- [4] K. Abe *et al.*, Phys. Rev. D **87**, 092003 (2013).
- [5] T2K Collaboration, K. Abe *et al.*, Phys. Rev. D **87**, 012001 (2013).
- [6] D. Renker and E. Lorenz, Journal of Instrumentation **4**, P04004 (2009).
- [7] P.-A. Amaudruz *et al.*, Nuclear Instruments and Methods in Physics Research Section A: Accelerators, Spectrometers, Detectors and Associated Equipment **696**, 1 (2012).
- [8] N. Abgrall *et al.*, Nuclear Instruments and Methods in Physics Research Section A: Accelerators, Spectrometers, Detectors and Associated Equipment **637**, 25 (2011).
- [9] S. Assylbekov *et al.*, Nuclear Instruments and Methods in Physics Research Section A: Accelerators, Spectrometers, Detectors and Associated Equipment **686**, 48 (2012).
- [10] D. Allan *et al.*, Journal of Instrumentation **8**, P10019 (2013).
- [11] S. Aoki *et al.*, Nuclear Instruments and Methods in Physics Research Section A: Accelerators, Spectrometers, Detectors and Associated Equipment **698**, 135 (2013).
- [12] J. Estrada, C. Garcia, B. Hoeneisen, and P. Rubinov, (2003).
- [13] S. Fukuda *et al.*, Nuclear Instruments and Methods in Physics Research Section A: Accelerators, Spectrometers, Detectors and Associated Equipment **501**, 418 (2003).



# List of Figures

1.1	Schematic of the T2K experiment showing the near and far sites, separated by the the 295 km baseline. . . . .	3
1.2	The 68% and 90% confidence level allowed regions for $\sin^2 2\theta_{13}$ as a function of $\delta_{CP}$ for normal hierarchy (top) and inverted hierarchy (bottom) The solid line represents the best fit $\sin^2 2\theta_{13}$ for a given $\delta_{CP}$ . The shaded region shows the average $\theta_{13}$ provided by the reactor constraint [2].	4
1.3	A schematic of the T2K neutrino beamline (left) and a side view of the secondary beamline (right) [1]. . . . .	5
1.4	The POT recorded by CT5 as a function of time (blue line) and the recorded beam power in $\nu$ running mode (red dots) and $\bar{\nu}$ running mode (purple dots). . . . .	7
1.5	Muon neutrino survival probability at 295 km (top) and neutrino fluxes for different off-axis angles (bottom) [5]. The peak neutrino lowers and the energy distribution narrows as the off-axis angle increases. . . . .	8
1.6	A schematic of INGRID [1]. . . . .	9
1.7	An exploded view of ND280 [1]. . . . .	10
1.8	Example of reconstructed T2K events in SK for a muon-like ring (left) and an electron-like ring (right) [1]. . . . .	16



# List of Tables

1.1	Summary of the ECal design showing the overall dimensions, numbers of layers, length and orientation of the scintillator bars, numbers of bars, and lead thickness for each module [10]. . . . .	13
-----	--	----